

Fracture of brittle materials: effects of test method and threshold stress on the Weibull modulus

P.D. Warren¹

Pilkington plc, Hall Lane, Lathom, Ormskirk L40 5UF, UK

Received 14 July 1997; received in revised form 31 May 2000; accepted 4 June 2000

Abstract

The cumulative probability of failure of a brittle material during loading can be related to the mean number of flaws in the body that are critical, i.e. satisfy some fracture criterion. Here, this approach is related to the more conventional Weibull statistics via Wilshaw's concept of a searched area. A power-law function for the flaw distribution is assumed and also the existence of a maximum crack size, and hence a threshold stress. The Weibull modulus, m , is regarded as a quantity that may vary with stress. It is shown that $m(\sigma) = [\sigma/N(\sigma)][dN(\sigma)/d\sigma]$ where σ is the stress and $N(\sigma)$ is the appropriate number of critical flaws. Quantitative expressions for $m(\sigma)$ are derived for tension tests, three-point bend tests, four-point bend tests and Hertzian indentation. It is shown that these test methods may all give different values for the Weibull modulus even though the flaw distribution remains the same. © 2001 Elsevier Science Ltd. All rights reserved.

Keywords: Failure probability; Fracture; Mechanical properties; Test methods; Weibull modulus

1. Introduction

Brittle materials (those with fracture toughness below $\approx 20 \text{ MPa m}^{1/2}$) show a variability in strength because of the presence of a distribution of cracks — both in size and position. These cracks can arise from a number of causes: surface cracks can arise from handling damage, or internal cracks can arise from processing defects such as pores. Weibull¹ introduced a simple mathematical function that is capable of describing the variability in strength. The cumulative probability that a body fails during stressing in uniform tension up to a stress σ , $F(\sigma)$, is given by:

$$F(\sigma) = 1 - \exp\left[-\left(\frac{\sigma}{\sigma_0}\right)^m\right] \quad (1)$$

σ_0 is a normalising parameter and m is a constant known as the Weibull modulus. It is frequently assumed that the Weibull modulus has no physical significance.

An alternative formula has been derived by Danzer² who showed that the cumulative failure probability $F(\sigma)$ was given by:

$$F(\sigma) = 1 - \exp[-N(\sigma)] \quad (2)$$

where $N(\sigma)$ is the mean number of critical flaws one would expect to find in a specimen during loading to σ . A critical flaw is one which satisfies some fracture criterion — for instance $K_I > K_{IC}$ would be the simplest such criterion. (Clearly any given specimen cannot contain more than 1 such critical flaw for a given loading arrangement.) It should be emphasised that Weibull's and Danzer's approach to flaw statistics are both based on "weakest link statistics" so that failure of one element of a body leads to failure of the whole body. As such, this approach cannot be used to describe (i) fracture in materials which exhibit R -curve behaviour or (ii) fracture in stabilising stress fields. In both of these cases stable crack growth may occur so that the flaw distribution when fracture occurs is not the same as the initial flaw distribution. Nor can the weakest link approach be used directly to describe constrained cracking — such as occurs in brittle coatings or in the fragmentation of brittle fibres in composite materials. In these cases a

¹ Formerly at the Department of Materials, Leeds University, Leeds LS2 9HT, UK.

E-mail address: paul.warren@ptc.pilkington.co.uk.

given fracture event may be dependent on the whole history of fracture.

In this paper a weakest link approach is assumed to be valid and Weibull's Eq. (1), is combined with Danzer's Eq. (2). Only surface-breaking flaws are considered — i.e. those likely to have arisen from surface damage or machining.

2. Calculating the Weibull modulus, m

2.1. The physical significance of m

Equating Eqs. (1) and (2):

$$F(\sigma) = 1 - \exp\left[-\left(\frac{\sigma}{\sigma_0}\right)^m\right] = 1 - \exp[-N(\sigma)] \quad (3a)$$

Equating terms in the square brackets, taking logarithms and differentiating:

$$m(\sigma) = \frac{\sigma}{N(\sigma)} \frac{dN(\sigma)}{d\sigma} \quad (3b)$$

where the Weibull modulus, $m(\sigma)$, is regarded as a quantity which may vary with stress.

Eq. (3b) demonstrates that the Weibull modulus is related to the rate at which cracks become critical with stress compared to the number of cracks that are already critical. Clearly, $m(\sigma)$ is the slope of the curve resulting from a plot of $\ln[-\ln[1-F(\sigma)]]$ versus $\ln(\sigma)$ but $m(\sigma)$ is the local slope of such plots.

It should be noted that the expression given for the failure probability, Eq. (1), is the simplest possible version: it assumes that the stress state is uniform tension and does not allow for specimens of different dimensions. For stress fields that are inhomogeneous over a surface the stress can be written

$$\sigma(x, y) = \sigma_n f(x, y) \quad (3c)$$

where σ_n is some nominal stress (usually the maximum surface stress) that is characteristic of the inhomogeneous stress field and $f(x, y)$ describes the spatial variation of the stress field. Stanley et al.,³ showed that the most general form of the expression for failure probabilities is:

$$F(\sigma_n) = 1 - \exp\left[-\left(\frac{\sigma_n}{\sigma_u}\right)^m \Gamma\left(1 + \frac{1}{m}\right) \frac{A}{A_0} \Sigma A\right] \quad (3d)$$

where σ_u is the unit strength — that is, the strength of a specimen of unit area, A_0 , measured in uniform tension; $\Gamma()$ is the gamma function; A is the area of the specimen under tension and ΣA is the stress-area integral, defined as:

$$\Sigma A = \int_A [f(x, y)]^m dx dy \quad (3e)$$

In this case, the expression for the Weibull modulus becomes

$$m(\sigma_n) = \frac{\sigma_n}{N(\sigma_n)} \frac{dN(\sigma_n)}{d\sigma_n} \quad (3f)$$

2.2. Searched areas, $A(\sigma_n, c)$

To proceed, $N(\sigma_n)$ must be calculated. For surface-breaking flaws Wilshaw⁴ introduced the concept of “searched area”, $A(\sigma_n, c)$. The searched area is that area of surface within which $K_I \geq K_{Ic}$ (for a crack of size c) during loading to σ_n . $n(c)$ is defined as the number of flaws per unit area per unit flaw size range, in which case the expression for $N(\sigma_n)$ is:

$$N(\sigma_n) = \int_{c_{\min}}^{c_{\max}} A(\sigma_n, c) n(c) dc \quad (4)$$

where c_{\min} and c_{\max} are the sizes of the smallest and largest crack that can be propagated by a stress σ_n . Clearly c_{\min} must be determined from σ_n via some fracture mechanics relationship, but c_{\max} may, in theory, tend to infinity. In reality, however, there must be an upper limit to c_{\max} — for example, no specimen can contain a flaw larger than the specimen itself. If the number of critical flaws cannot be expressed as an analytical function of the searched area then discrete summation must be used to calculate $N(\sigma_n)$.

2.3. The flaw distribution, $n(c)$

With an expression for $n(c)$, $m(\sigma_n)$ can be evaluated for a variety of cases. For simplicity it is assumed here that $n(c) = \beta c^{-r}$. The question of what a typical flaw distribution is in practice, however, remains undecided; in particular, it is the form of the function for small cracks that is particularly uncertain. There are two reasons for this: (i) if one is only interested in the strength of a ceramic component then it is the large flaws that are of concern, and (ii) for most test methods (although not Hertzian indentation) fracture occurs by the propagation of the largest flaws — so that information about the small-crack end of the distribution can only be obtained by testing very small specimens. The number of direct determinations of flaw distributions is very small. Previous work has included that by Wilshaw,⁴ Argon,⁵ Polinieccki and Wilshaw,⁶ Matthews et al.⁷ and Evans and Jones.⁸ In these cases the flaw distribution was found to be predominantly a decreasing function of crack size i.e. a high density of small flaws and lower densities of larger flaws, although in the results of

Matthews et al.⁷ there was evidence of local maxima in the flaw density at intermediate flaw sizes. More recent work by Santhanam and Shaw⁹ determined flaw distributions by forcing a fit of experimental data to an equation of the form $n(c) = \frac{k^{r-1}}{(r-2)} c^{-r} e^{-k/c}$. This automatically causes the density of small cracks to be small. Sigl¹⁰ studied the effects of multiple flaw populations, all distributed according to a gamma-distribution; again, this distribution automatically forces the density of small cracks to be small. Warren,¹¹ showed how to determine the flaw distribution *without* making prior assumptions about its form; experimental determination of surface flaw densities,¹² in abraded and polished aluminas revealed again that the density of cracks decreased monotonically as the crack size increased. Work remains to be done in this area: the experimental evidence referred to above, however, certainly suggests that the density of small flaws increases as the flaw size decreases.

Assuming that $n(c) = \beta c^{-r}$ four experimental situations are studied: uniform tension, three-point bending, four-point bending and Hertzian indentation.

2.4. The tension test

For a uniform tension test a bar is pulled at both ends by a load P ; the cross-sectional area of the bar normal to the load is w^2 and the length of the bar is L . A tensile stress $\sigma_n = P/w^2$ results. The mode I stress intensity factor is $K_I = Y\sigma_n(\pi c)^{1/2}$ where Y is a crack shape parameter. For a crack of a given size there is a minimum stress necessary to cause fracture, $\sigma_{\min} = \delta/c^{1/2}$ where $\delta = K_{IC}/Y\pi^{1/2}$. For a given fracture stress σ_n there is a lower limit to the size of crack that can be propagated, $c_{\min} = (\delta/\sigma_n)^2$; if there is an upper limit to the flaw size distribution, c_{\max} , then there is an absolute lower limit to the fracture stress, $\sigma_L = \delta/c_{\max}^{1/2}$. Assuming that $\sigma_n \geq \sigma_{\min}$ and also assuming that all the flaws are oriented perpendicular to the applied stress then the searched area is clearly:

$$A(\sigma_n, c) = 4wL \tag{5a}$$

and the number of critical flaws is:

$$\begin{aligned} N(\sigma_n) &= \int_{c_{\min}}^{c_{\max}} 4wL\beta c^{-r} dc \\ &= \frac{4wL\beta}{(r-1)\delta^{2r-2}} (\sigma_n^{2r-2} - \sigma_L^{2r-2}) \end{aligned} \tag{5b}$$

The Weibull modulus derived from Eq. (3b) is therefore:

$$m(\sigma_n) = \frac{2r-2}{1 - (\sigma_n/\sigma_L)^{-2r+2}} \tag{5c}$$

A number of points are worthy of note. If there is no upper limit to the flaw size, c_{\max} , then σ_L tends to 0 and so $m(\sigma_n)$ tend to $2r-2$ — a result that has been derived before.¹³ If there *is* an upper limit to the flaw distribution then $m(\sigma_n)$ is greater than $(2r-2)$ — i.e. the slope of a Weibull plot should be increased for stresses close to the threshold fracture stress: this is as observed in practice.¹⁴ For values of σ_n/σ_L close to 1, $m(\sigma_n)$ tends to infinity for any value of r . Numerical fitting of Eq. (5c) to experimental data can be used to obtain the values of r and σ_L and hence the value of m to be expected if there were no threshold stress. Finally, the functional form of the expression for $N(\sigma_n)$, Eq. (5b), suggests that the conventional way of constructing a 3-parameter Weibull plot (i.e. to account for the existence of a threshold stress) may be inappropriate. For a 3-parameter Weibull distribution one usually plots $\ln[-\ln[1 - F(\sigma_n)]]$ vs. $\ln(\sigma_n - \sigma_L)$: Eq. (5b) suggests that a more sensible ordinate would be $\ln(\sigma_n^m - \sigma_L^m)$. This point was first made by Matthewson,¹⁵ but appears not to have been adopted since.

2.5. The three-point bend test

A load P is applied to a bar of width b , thickness h in a three-point bend configuration where $2L$ is the distance between the supports. σ_n is the maximum stress in the bar, $\sigma_n = 3PL/bh^2$ and σ_{nL} is the lower limit to this maximum stress, $\sigma_{nL} = \delta/c_{\max}^{1/2}$ with δ as before. The searched area is given by Warren:¹¹

$$A(\sigma_n, c) = bL(1 - \delta/\sigma_n c^{1/2}) \tag{6a}$$

Using the same approach as above it is straightforward to show that the expression for $N(\sigma_n)$ is:

$$\begin{aligned} N(\sigma_n) &= \frac{2bL\beta(\sigma_n^{2r-2} - (2r-1)\sigma_{nL}^{2r-2} + (2r-2)\sigma_{nL}^{2r-1}/\sigma_n)}{(r-1)(2r-1)\delta^{2r-2}} \end{aligned} \tag{6b}$$

The Weibull modulus is:

$$\begin{aligned} m(\sigma_n) &= \frac{(2r-2) - (2r-2)(\sigma_n/\sigma_{nL})^{-2r+1}}{1 - (2r-1)(\sigma_n/\sigma_{nL})^{-2r+2} + (2r-2)(\sigma_n/\sigma_{nL})^{-2r+1}} \end{aligned} \tag{6c}$$

If $\sigma_{nL} = 0$ then $m(\sigma_n) = 2r-2$. Again, if there is a threshold stress then the Weibull modulus increases for stresses close to this value.

2.6. The four-point bend test

A load P is applied to a bar of width b , thickness h in a four-point bend configuration where $2L$ is the distance between the outer supports and 2ℓ the distance between the inner supports. σ_n is the maximum stress in the bar, $\sigma_n = 3P(L - \ell)/bh^2$ and σ_{nL} is the lower limit to this maximum stress, $\sigma_{nL} = \delta/c_{\max}^{1/2}$ with δ as before. The searched area is given by:

$$A(\sigma_n, c) = 2bL \left[1 - \frac{\delta}{\sigma_n \sqrt{c}} \left(1 - \frac{\ell}{L} \right) \right] \quad (7a)$$

$N(\sigma_n)$ is given by:

$$N(\sigma_n) = \frac{2bL\beta \left[(1 + \ell(2r - 2)/L)\sigma_n^{2r-2} - (2r-1)\sigma_{nL}^{2r-2} + (2r-2)(1 - \ell/L)\sigma_{nL}^{2r-1}/\sigma_n \right]}{(r-1)(2r-1)\delta^{2r-2}} \quad (7b)$$

The Weibull modulus is:

$$m(\sigma_n) = \frac{(2r-2)(1 + \ell(2r-2)/L) - (2r-2)(1 - \ell/L)(\sigma_n/\sigma_{nL})^{2r+1}}{(1 + \ell(2r-2)/L) - (2r-1)(\sigma_n/\sigma_{nL})^{-2r+2} + (2r-2)(1 - \ell/L)(\sigma_n/\sigma_{nL})^{-2r+1}} \quad (7c)$$

If $\sigma_{nL} = 0$ then $m(\sigma_n) = 2r - 2$ as before. If $\ell/L = 0$ (i.e. a three-point bend test) then Eqs. (7b,c) become identical with Eqs. (6b,c) as a special case.

Plots of Eqs. (5c), (6c) and (7c) are shown in Figs. 1(a–c) for three different values of r . These figures are discussed below.

2.7. The Hertzian indentation test

In Hertzian indentation a hard sphere of radius R is pressed into the surface of a material under a load P . At a sufficiently large load a pre-existing crack of depth c will begin to grow to give the characteristic ring-crack or ring/cone-crack system.¹⁶ In what follows the stress driving fracture is assumed to be the *surface* radial stress, i.e. the steep stress gradients present in the Hertzian field,^{16,17} are ignored. This is acceptable when large spheres are used to indent well polished surfaces; a quantitative analysis of what constitutes a large sphere and a well polished surface is presented in reference.¹⁷

3. Weibull modulus as a function of load

Results for Hertzian indentation will be given in terms of both loads and stresses. For tension or bending tests variations in fracture load may arise from variations in specimen dimensions as well as from variations in material strength. Therefore, fracture load is not a

suitable variable for failure statistics. For Hertzian indentation this is not the case: variations in fracture load are directly related to variations in material strength. Furthermore, because the relation between maximum stress and load in Hertzian indentation is non-linear (see below) some differences in calculations of the Weibull modulus arise. In terms of load, the searched area $A(P, c)$ is clearly that area of surface within which $K_I \geq K_{Ic}$ (for a crack of size c) during loading to P . The number of critical flaws, $N(P)$, is:

$$N(P) = \int_{c_{\min}}^{c_{\max}} A(P, c)n(c)dc \quad (8a)$$

The Weibull modulus is given by:

$$m(P) = \frac{P}{N(P)} \frac{dN(P)}{dP} \quad (8b)$$

4. Hertzian indentation

Contact of the sphere and substrate occurs over a circular patch, radius a , given by:

$$a = (3RP/4E^*)^{1/3} \quad (9a)$$

where $1/E^* = (1 - \nu_1^2)/E_1 + (1 - \nu_2^2)/E_2$ and ν_1, ν_2 , and E_1, E_2 are the Poisson's ratios and Young moduli of the sphere and substrate respectively. The radial component of stress is tensile outside the contact patch and of magnitude $\sigma_{rr} = (1 - 2\nu)P/2\pi r^2$ where r is the distance from the centre of the contact, $r \geq a$. Define $\gamma = 3R/4E^*$ and $\delta = K_{Ic}/Y\pi^{1/2}$, as before. The maximum value of the radial stress clearly occurs at $r = a$ and is given by:

$$\sigma_n = \frac{(1 - 2\nu)P^{2/3}}{2\pi\gamma^{2/3}} \quad (9b)$$

The maximum distance, r_{\max} , a crack of size c can be situated from the centre of the contact and still be critical under a maximum stress σ_n (or load P) is:

$$r_{\max}^2 = \left(\frac{1 - 2\nu}{2\pi} \right) \frac{Pc^{3/2}}{\delta} = \left(\frac{2\pi\gamma}{1 - 2\nu} \right)^2 \frac{\sigma_n^3 c^{3/2}}{\delta} \quad (9c)$$

For a maximum stress σ_n (or load P) the size of the smallest crack that can be detected is:

$$c_{\min} = \left(\frac{2\pi\delta}{1 - 2\nu} \right)^2 \frac{\gamma^{4/3}}{P^{2/3}} = \left(\frac{\delta}{\sigma_n} \right)^2 \quad (9d)$$

At a maximum stress σ_n one might expect the searched area to be given by:

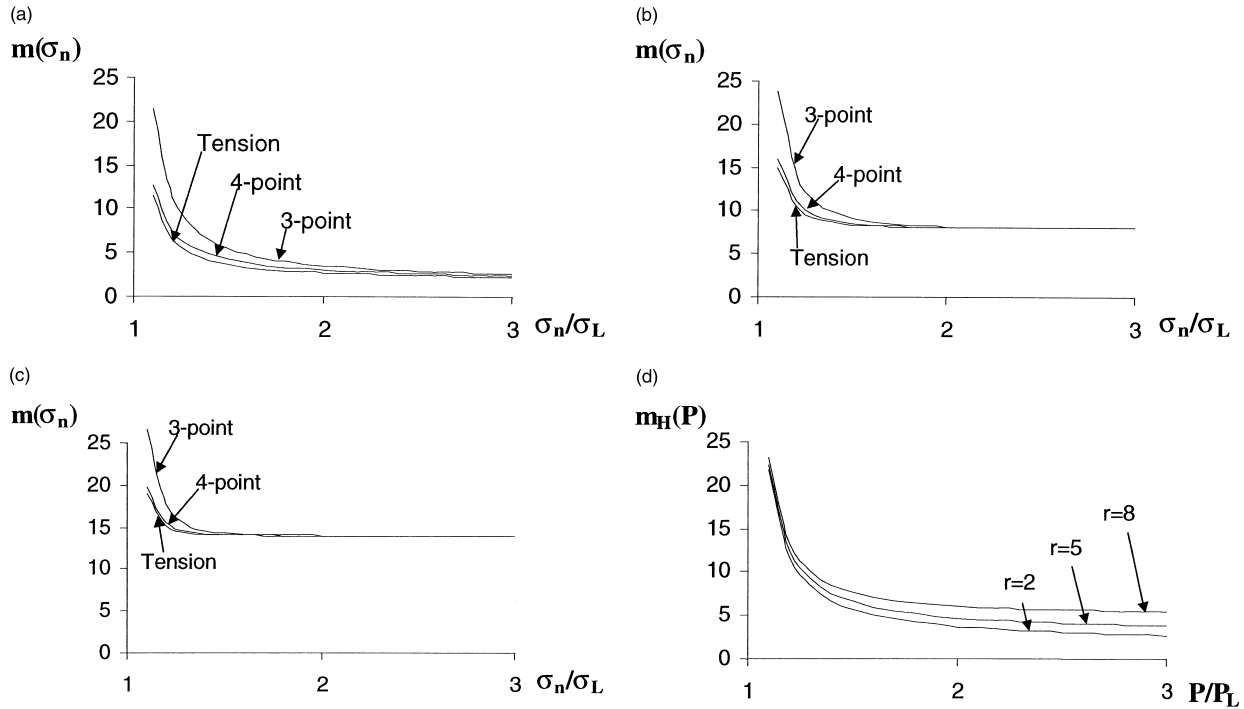


Fig. 1. Plot of Weibull modulus $m(\sigma_n)$ as a function of σ_n/σ_L for tension tests, three-point bend tests and four-point bend tests, (a) $\ell/L = 0.25$, $r = 2$; (b) $\ell/L = 0.25$, $r = 5$; (c) $\ell/L = 0.25$, $r = 8$; (d) plot of Hertzian Weibull modulus, $m_H(P)$ as a function of P/P_L for three different values of r .

$$A^*(\sigma_n, c) = \pi(r_{\max}^2 - a^2) = \pi \left(\frac{2\pi\gamma}{1-2\nu} \right)^2 \left(\frac{\sigma_n^3 c^{1/2}}{\delta} - \sigma_n^2 \right) \quad (10a)$$

or in terms of the load P :

$$A^*(P, c) = \pi(r_{\max}^2 - a^2) = \pi \left(\left(\frac{1-2\nu}{2\pi} \right) \frac{Pc^{1/2}}{\delta} - \gamma^{2/3} P^{2/3} \right) \quad (10b)$$

However, as shown by Wilshaw,⁴ Eqs. (10a,b) are not expressions for the area searched *up to* a stress σ_n or load P . They are, rather, expressions for the area searched *at* a stress σ_n or load P . A crack of size c can be detected at all stresses above $\sigma_{n\min}$ or loads above P_{\min} where:

$$\sigma_{n\min} = \frac{\delta}{c^{1/2}} \quad (10c)$$

Using Eq. (9d) the expression for P_{\min} is:

$$P_{\min} = \frac{\gamma^2}{c^{3/2}} \left(\frac{2\pi\delta}{1-2\nu} \right)^3 \quad (10d)$$

and the expression for the corresponding minimum contact radius a_{\min} is:

$$a_{\min} = \frac{2\pi\gamma}{1-2\nu} \frac{\delta}{c^{1/2}} \quad (10e)$$

The correct expressions for the area searched *up to* a stress σ_n or load P are, therefore:¹¹

$$A(\sigma_n, c) = \pi(r_{\max}^2 - a_{\min}^2) = \pi \left(\frac{2\pi\gamma}{1-2\nu} \right)^2 \left(\frac{\sigma_n^3 c^{1/2}}{\delta} - \frac{\delta^2}{c} \right) \quad (11a)$$

$$A(P, c) = \pi(r_{\max}^2 - a_{\min}^2) = \pi \left(\frac{2\pi\gamma}{1-2\nu} \right)^2 \left(\left(\frac{1-2\nu}{2\pi} \right) \frac{Pc^{1/2}}{\delta} - \frac{\delta^2}{c} \right) \quad (11b)$$

Substituting Eq. (11a) into Eq. (4), the number of critical cracks during loading up to a stress σ_n is:

$$N(\sigma_n) = \frac{\pi\beta\gamma^2}{r(r-3/2)\delta^{2r-2}} \times \left(\frac{2\pi}{1-2\nu} \right)^2 \left(\frac{3\sigma_n^{2r}}{2} + \left(r - \frac{3}{2} \right) \sigma_L^{2r} - r\sigma_n^3 \sigma_L^{2r-3} \right) \quad (11c)$$

and substituting Eq. (11b) into Eq. (8a) the number of critical cracks during loading up to a load P is:

$$N(P) = \frac{\pi\beta\gamma^{(2-4r)/3}}{r(r-3/2)\delta^{2r-2}} \left(\frac{2\pi}{1-2\nu}\right)^{2-2r} \left(\frac{3P^{2r/3}}{2} + \left(r - \frac{3}{2}\right)P_L^{2r/3} - rPP_L^{(2r-3)/3}\right) \quad (11d)$$

where σ_{nL} is the threshold maximum Hertzian stress. It should be noted that the expressions for $N(\sigma_n)$ and $N(P)$ are independent of the area of the specimen. As the area of a brittle material increases, the probability of finding both large and small cracks increases. Tension and bending tests will sample the larger end of the flaw distribution whereas Hertzian indentation finds flaws within a size range determined largely by the size of the sphere used, Roberts.¹⁸ Increasing the size of the specimen thus has no effect on the failure probabilities for Hertzian indentation.

The Hertzian Weibull moduli derived from Eqs. (11c,d) are:

$$m_H(\sigma_n) = \frac{6r(1 - (\sigma_n/\sigma_L)^{-2r+3})}{3 + (2r-3)(\sigma_n/\sigma_L)^{-2r} - 2r(\sigma_n/\sigma_L)^{-2r+3}} \quad (11e)$$

and

$$m_H(P) = \frac{2r(1 - (P/P_L)^{(-2r+3)/3})}{3 + (2r-3)(P/P_L)^{-2r/3} - 2r(P/P_L)^{(-2r+3)/3}} \quad (11f)$$

For a conventional tension or bending test, assuming no threshold stress, the Weibull modulus should be $m = 2r - 2$. Eqs. (11e,f) shows that the Hertzian Weibull modulus is $m_H(\sigma_n) = 2r$, assuming no threshold stress, or $m_H(P) = 2r/3$, assuming no threshold load. Hence, the relation between the Weibull modulus measured conventionally and the Hertzian Weibull modulus is $m = m_H(\sigma_n) - 2$ or $m = 3m_H(P) - 2$. Confirmation of this prediction is provided by experimental results of Hertzian tests on glass, Figs. 2a and b. The tests were performed on both the air-side and the tin-side of as-received specimens of float glass, using a WC-Co sphere of radius 1 mm. Ninety tests were done in all. The Weibull modulus determined from the fracture loads is ~ 2.5 ; one, therefore, predicts a Weibull modulus of 5.5 for the same glass but determined by more conventional tests, assuming that $P_L = 0$. For similar glass plates tested in burst tests, the Weibull modulus is “usually between 5 and 6.”¹⁹ The fracture loads for the tin-side are lower than those for the air-side. This difference is usually attributed to the fact that the tin-side of the glass may suffer more surface damage than the air-side during production as a result of contact with transport rollers in the lehr.

5. Discussion

A number of points are worth discussing. Fig. 1a, b and c compare the Weibull moduli determined from three different test methods: tension, 3-point bending and 4-point bending. Eqs. (5c), (6c) and (7c) show that if there is no threshold stress then all three methods will give the same value for the Weibull modulus. If there is a maximum crack size and hence a threshold stress the three different test methods may give rise to different values for the Weibull moduli — depending on what section of the flaw distribution is being sampled. Clearly, the effects are most noticeable for fracture stresses close to the threshold, implying that the effects will become more noticeable as the specimen size increases. Fig. 1a, b and c also shows that the biggest increases in Weibull modulus are to be expected for the three-point bend test and the smallest changes for the tension test. This is related to the fact that the stress is wholly non-uniform in the three-point test and wholly uniform in the tension test, with the four-point test being intermediate in its degree of stress uniformity.

The most surprising results of this paper relate to the Hertzian test. There are two points of note. First, because of the non-linear relation between maximum stress and load there is a difference in the values of Weibull modulus determined from stress, Eq. (11e), compared to that determined from load, Eq. (11f). Because the maximum stress is proportional to the cube root of the load there is a factor of 3 difference between the two sets of Weibull moduli. Secondly, the r -dependence of the Weibull modulus determined from stress [Eq. (11e)] is different for the Hertzian case compared to the three other methods. A conventional Weibull analysis of the Hertzian test confirms these results, Rickerby.²⁰ This is demonstrated as follows.

For a radial stress field, Weibull’s expression for the cumulative failure probability is:

$$F(\sigma) = 1 - \exp\left[-\int_r \left(\frac{\sigma_{rr}}{\sigma_o}\right)^m \frac{2\pi r dr}{A_o}\right] \quad (12a)$$

Rickerby (his equation 17) showed that the resulting expression for the failure probabilities is:

$$F(\sigma_n) = 1 - \exp\left(\frac{-\pi a^2}{A_o} \left(\frac{3m}{(m-1)(m+2)}\right) \left(\frac{\sigma_n}{\sigma_o}\right)^m\right) \quad (12b)$$

where a is the contact radius corresponding to the maximum stress σ_n . But, from Eq. (9a,b) an expression for the contact radius, a , when the maximum stress is σ_n is:

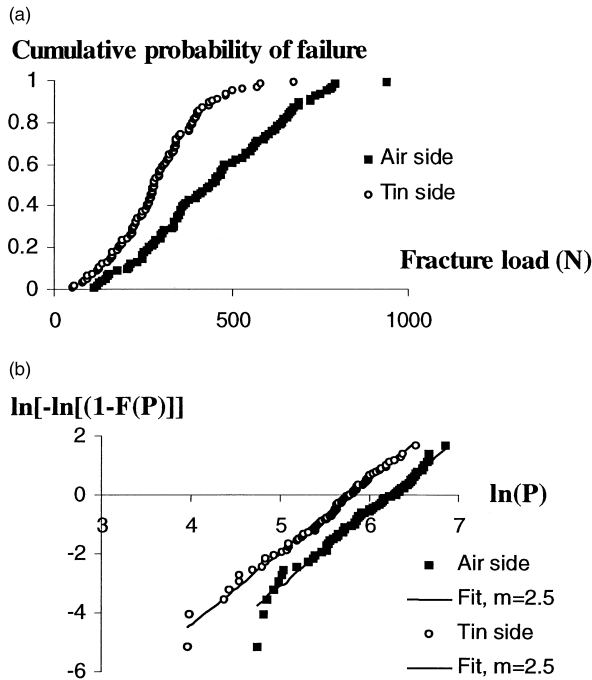


Fig. 2. Results for Hertzian indentation of both the air-side and the tin-side of as-received float glass. (a) Plot of cumulative probability of fracture vs. fracture load, (b) Weibull plot of the data using fracture load as the variable. The Hertzian Weibull modulus, m_H , is ~ 2.5 for both sides of the glass. A tungsten carbide sphere of radius 1 mm was used for the tests.

$$a = \frac{2\pi\gamma\sigma_n}{1-2\nu} \quad (12c)$$

in which case:

$$F(\sigma_n) = 1 - \exp\left(\frac{-4\pi^3\gamma^2\sigma_n^2}{(1-2\nu)^2 A_0} \left(\frac{3m}{(m-1)(m+2)}\right) \left(\frac{\sigma_n}{\sigma_0}\right)^{m+2}\right) \quad (12d)$$

Thus, conventional Weibull analysis (with stress as the variable) confirms that (i) the failure probability for Hertzian indentation is independent of the size of the specimen, and (ii) the slope of a Weibull plot will be $m+2$, not m .

The underlying reason for the differences in Weibull moduli for the 4 different test methods lies in the different functional forms for the searched area as a function of stress. For the tension test, Eq. (5a), the searched area is constant; for a three-point bend test, Eq. (6a), the searched area rises from zero asymptotically towards a limit; for the four-point bend test, Eq. (7a), the searched has a constant component and a rising component; for the Hertzian test, Eq. (11a,b), the searched area increases without limit as the stress (load) is increased.

6. Conclusions

A general method for relating the Weibull modulus $m(\sigma_n)$ to the flaw population of a brittle material has been demonstrated. Using a simple power-law representation for the flaw distribution it has been shown that the Weibull modulus determined from tension tests, three-point bend tests and four-point bend tests will be the same if there is no threshold stress for fracture; if such a threshold stress does exist then the different test methods will give different values for the Weibull modulus. Furthermore, the relationship between the Weibull modulus determined from Hertzian indentation tests has been related to that measured in more conventional fracture tests. Further work will investigate this approach assuming different functional forms for the flaw distribution.

Acknowledgements

Parts of this work were supported under the EPSRC/LINK Nanotechnology Project Characterisation of surface roughness and sub-surface damage. The author would also like to thank Dr. S.G. Roberts for a critical reading of the manuscript.

References

1. Weibull, W., A statistical distribution function of wide application. *J. Appl. Mech.*, 1951, **18**, 293–297.
2. Danzer, R., A general strength distribution function for brittle materials. *J. Eur. Ceram. Soc.*, 1992, **10**, 461–472.
3. Stanley, P., Fessler, H. and Sivill, A. D., An engineer's approach to the prediction of failure probability of brittle components. *Proc. Brit. Ceram. Soc.*, 1973, **22**, 453–487.
4. Wilshaw, T. R., The Hertzian fracture test. *J. Phys. D: Appl. Phys.*, 1971, **4**, 1567–1581.
5. Argon, A. S., Distribution of cracks on glass surfaces. *Proc. Roy. Soc.*, 1959, **A250**, 482–492.
6. Poloniecki, J. D. and Wilshaw, T. R., Determination of surface crack size densities in glass. *Nature London*, 1971, **229**, 226–227.
7. Matthews, J. R., McClintock, F. A. and Shack, W. J., Statistical determination of surface flaw density in brittle materials. *J. Am. Ceram. Soc.*, 1976, **59**, 304–308.
8. Evans, A. G. and Jones, R. I., Evaluation of a fundamental approach for the statistical analysis of fracture. *J. Am. Ceram. Soc.*, 1978, **61**, 156–160.
9. Santhanam, S. and Shaw, M. C., Determination of the flaw-size distribution by the crack-off process. *J. Am. Ceram. Soc.*, 1990, **73**, 2922–2925.
10. Sigl, L. S., Effects of the flaw distribution function on the failure probability of brittle materials. *Z. Metallkd.*, 1992, **83**, 518–523.
11. Warren, P. D., Statistical determination of surface flaw distributions in brittle materials. *J. Eur. Ceram. Soc.*, 1995, **15**, 385–394.
12. Warren, P. D., Kolosov, O. V., Roberts, S. G. and Briggs, G. A. D., Characterization of surface damage via surface probes. *Nanotechnology*, 1996, **7**, 288–294.
13. Jayatilaka, A. De. S. and Trustrum, K., Statistical approach to brittle fracture. *J. Mater. Sci.*, 1977, **12**, 1426–1430.

14. Seidel, J., Claussen, N. and Riedel, J., Reliability of alumina ceramics: effect of grain size. *J. Eur. Ceram. Soc.*, 1995, **15**, 395–404.
15. Matthewson, M. J., An investigation of the statistics of fracture. In *Strength of Inorganic Glass*, ed. C. R. Kurkijian, Plenum Press, 1985, pp. 429–442.
16. Frank, F. C. and Lawn, B. R., On the theory of Hertzian fracture. *Proc. R. Soc. Lond.*, 1967, **A229**, 291–306.
17. Warren, P. D., Hills, D. A. and Roberts, S. G., Surface flaw distributions in brittle materials and Hertzian fracture. *J. Mater. Res.*, 1994, **9**, 3194–3202.
18. Roberts, S. G., Hertzian testing of ceramics. *Proceedings of the British Ceramic Society*, in press.
19. Dr. J. Bradshaw, Pilkington plc, Private communication.
20. Rickerby, D. G., Theoretical aspects of the statistical variation of strength. *J. Mater. Sci.*, 1980, **15**, 2466–2470.